Air Flow Exchange Velocity of Urban Canyon Cavities due to Thermal Spatial Differences

Marta Oliveira Panão[1], Helder Gonçalves[1] and Paulo Ferrão[2]

[1] Renewable Energy Department, INETI, Lisbon, Portugal
[2] IN+, Center for Innovation, Tech. and Policy Research, IST, Lisbon, Portugal

ABSTRACT: In this paper, the air exchange velocity between the urban canyon cavity and the air layer above roof level is quantified, using a two-dimensional k-ε model, and correlated with the air cavity mean temperature, for two cases: leeward and downward wall heating. The spatial thermal differences are evaluated by assuming a wall temperature higher than the air temperature, with this difference ranging between 0 and 16 K. The undisturbed wind velocity above the roof level is varied from 1 to 6 ms^{-1} and the canyon aspect ratio is 1.5, which corresponds to a skimming flow regime.
The model predicts two situations, which correspond to air flow regimes where one or two eddies are formed, respectively: (a) for high wind speed, the air inside the cavity is negligible affect by the buoyancy effect and the air exchange velocity linearly increases with the increase of wind velocity; (b) for low wind speed, when the buoyancy forces are stronger than the wind induced forces, the air exchange velocity is not a linear function with the wind velocity. The transition wind velocity between (a) and (b) is a function of the wall-air temperature difference. The situation of windward heated wall and two eddies air flow regime is the most favorable to extract heat from the cavity. On the contrary, the heated air is hardly extracted from the cavity when only the wind induced eddy is predicted and windward wall is heated. In this situation an increase of 10 K on the wall temperature increases by 1 K the in-cavity air temperature.

Keywords: exchange velocity, heated surfaces, urban street canyon, urban cavity

1. INTRODUCTION

During a one day period, the urban canyon walls have different temperature patterns, mainly due to the sun incidence, which influence the air flow inside the cavity [1-2]. For a skimming flow regime [3], the in-cavity air is highly isolated from the external space by the formation of one (or more) vortices, promoting the accumulation of heat on the cavity, desirable on winter but not in summer. In pollution studies the removal rate of pollutant concentrations is measured by the air exchange rate (ACH) [4] which quantifies the air flux crossing the urban canyon top surface.

The spatial thermal differences among cavity surfaces contributes to reinforce the existent vortices or to form additional ones. These air flow exchanges result from the balance between buoyancy and advective forces.

In this paper the air exchange velocity is studied, which is related to the ACH by the width cavity, using the numerical predictions of a bi-dimensional k-ε turbulence model. The goal of this study is twofold: (1) estimating the air exchange velocity to analyse the walls thermal difference influence on the air flow regime inside the cavity; and (2) correlating it with the mean temperature of the urban cavity air.

2. MODEL FORMULATION

The turbulent flow field inside the urban cavity is calculated from the solution of the two-dimensional, steady-state, Reynolds-averaged Navier-Stokes equations by use of the original TEACH code [5], where thermal effects are included. The momentum, mass and thermal equations can be written in tensor notation, respectively, by:

$$u_j \frac{\partial u_i}{\partial x_j} = -\frac{1}{\rho}\frac{\partial p}{\partial x_i} + \nu \frac{\partial^2 u_i}{\partial x_j \partial x_j} - \frac{\partial \overline{u'_i u'_j}}{\partial x_j} - \frac{T - T_{ref}}{T} g_i \quad (1)$$

$$\frac{\partial u_i}{\partial x_i} = 0 \quad (2)$$

$$u_j \frac{\partial T}{\partial x_j} = \frac{\partial}{\partial x_j}\left(\frac{\nu_t}{\sigma_t} \frac{\partial T}{\partial x_j} \right) \quad (3)$$

where x_i are the Cartesian coordinates (x,z), u_i the components of the mean velocity (u,w), u_i' the fluctuations of the velocity components (u',w'), g_i the components of the gravitational acceleration (0,-g), p the mean pressure, T the absolute mean temperature, T_{ref} a reference temperature assumed here by the inflow air temperature, ρ (= 1.18 Kgm^{-3}) the air density at 300 K, ν (= 1.58×10^{-5} $m^2 s^{-1}$) the air kinematic viscosity at the same temperature, and σ_t (= 0.90) the turbulent Prandtl number. The Reynolds stress tensor components are estimated by the Boussinesq eddy viscosity:

$$-\overline{u_i'u_j'} = \nu_t\left(\frac{\partial u_i}{\partial x_j}+\frac{\partial u_j}{\partial x_i}\right)-\frac{2}{3}\delta_{ij}k \quad (4)$$

where δ_{ij} is the delta Kronecker function and ν_t the turbulent eddy viscosity calculated by the Prandtl-Kolmogorov relationship.

$$\nu_t = c_\mu \frac{k^2}{\varepsilon} \quad (5)$$

In the above expressions c_μ is a model constant (= 0.09), k is the turbulent kinetic energy and ε its dissipation rate which are calculated by solving the semi-empirical transport equations:

$$u_j\frac{\partial k}{\partial x_j} = \frac{\partial}{\partial x_j}\left(\frac{\nu_t}{\sigma_k}\frac{\partial k}{\partial x_j}\right)+G_k+I_k-\varepsilon \quad (6)$$

$$u_j\frac{\partial \varepsilon}{\partial x_j} = \frac{\partial}{\partial x_j}\left(\frac{\nu_t}{\sigma_\varepsilon}\frac{\partial \varepsilon}{\partial x_j}\right)+\frac{\varepsilon}{k}\left[c_{\varepsilon 1}\left(G_k+I_k\right)-c_{\varepsilon 2}\varepsilon\right] \quad (7)$$

with:

$$G_k = -\overline{u_i'u_j'}\frac{\partial u_i}{\partial x_j} \quad (8)$$

$$I_k = \frac{g_j}{T}\frac{\nu_t}{\sigma_t}\frac{\partial T}{\partial x_j} \quad (9)$$

and σ_k (= 1.0), σ_ε (= 1.3), $c_{\varepsilon 1}$ (= 1.44), $c_{\varepsilon 2}$ (= 1.92) constants of the model [1,2].

3. AIR EXCHANGE VELOCITY

The numerical model estimates for each point of the mesh the two mean air velocity x and z components, respectively, u and w. The fluctuation air velocity terms, u' and w', are obtained from the Reynolds stress tensor by (4).

The mean air flux, Φ_e, crossing the cavity top surface (surface S of Figure 1) is given by:

$$\Phi_e = \int_S\left(\overline{(w+w')^2}\right)^{1/2}dx \quad (10)$$

Because of mass conservation this term is numerically close to 0, thus, the air flux which enters (or exits) the cavity is defined by:

$$\Phi_e^+ = \frac{1}{2}\int_S\left(ww+\overline{w'w'}\right)^{1/2}dx \quad (11)$$

The fluctuating term of (11) is obtained by one of the components of the turbulent stress tensor:

$$\overline{w'w'} = \frac{2}{3}k-2\nu_t\frac{\partial w}{\partial z} \quad (12)$$

Numerically, each one of the terms w, k and ε is estimated for the surface S from the vertical average of the closest nodes j and j+1. The vertical gradient of w is estimated by:

$$\frac{\partial w}{\partial z} = \frac{w_{i,j+1}-w_{i,j}}{z_{i,j+1}-z_{i,j}} \quad (13)$$

The air exchange velocity is calculated from the ratio between the air exchange rate entering the cavity and the cavity width (W):

$$U_e = \frac{\Phi_e^+}{W} \quad (14)$$

Because the model mesh is uniform in the cavity area (see Figure 1), the difference between the air cavity mean temperature and the inflow air, ΔT_c, is calculated by the numerical average of the temperature difference on each node. The air velocity close to the wall, U_w, is calculated from the numerical average of $U = (u^2+w^2)^{1/2}$ for the set of nodes closest to the wall.

4. MODEL CHARACTERIZATION AND BOUNDARY CONDITIONS

The model calculates the air flow variables and the temperature for the geometry depicted on Figure 1 which dimensions are set to: building height (H) 60, cavity width (W) 40 and height of the roof level layer (z_δ) 100. The mesh, also depicted in Figure 1, is composed by two zones: the lower has a grid of 126×149 nodes and the upper 126×51.

The wind velocity at the inflow, u_{in}, in the region above z_r (= 10) is set with an undisturbed wind velocity value, U_0, which is a variable parameter ranging from 1 to 6 ms^{-1}. Below that level, u_{in} (w_{in} = 0) at the inflow varies with z according to:

$$u_{in}(z) = U_0\left(\frac{z-H}{z_r}\right)^{0.299} \quad \text{,if} \quad z-H < z_r \quad (15)$$

At the inflow, the turbulent kinetic energy and its dissipation rate were set to:

$$\kappa_{in} = 0.003u_{in}^2 \quad (16)$$

$$\varepsilon_{in} = \frac{c_\mu^{0.75}\kappa_{in}^{1.5}}{\kappa z} \quad (17)$$

with κ (= 0.40) the Von Karman constant.

No-slip boundary conditions are applied to building surfaces (roof, floor and walls) [6]. At the outflow, and upper boundary, the gradient of any variable is set to zero.

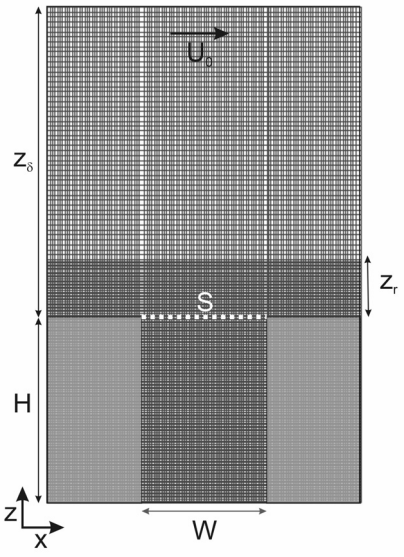

Figure 1: Model geometry and mesh characterization.

In terms of spatial thermal differences, three cases are considered: (1) inflow air and surfaces at

the same temperature (T = 293 K); (2) leeward surface temperature above inflow air temperature (Figure 2a); and (3) windward surface temperature above inflow air temperature (Figure 2b). The wall-air temperature difference (ΔT_w) ranges between 2 and 16 K, by steps of 2 K.

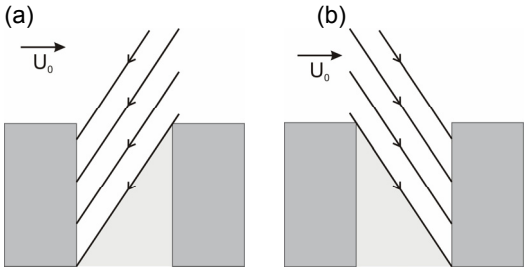

Figure 2: Solar incidence on urban cavity for (a) leeward heated wall and (b) windward heated wall.

5. AIR FLOW REGIMES AND AIR EXCHANGE VELOCITY

5.1 Case 0: Isothermal surfaces

For the studied geometry where the urban cavity has an aspect ratio (H/W) of 1.5 and both the air and surfaces are in isothermal conditions, only one eddy is formed inside the cavity and the air exchange velocity increases linearly with the undisturbed wind velocity, at a 4.1% rate (see 0 K line in Figure 3). The air velocity close to the surface, U_w also increases linearly with U_0 at a 22% rate, not shown here.

5.2 Case 1: Leeward heated surfaces

When leeward surface temperature is higher than air, the air close to the surface is heated and moves upwind, reinforcing the existent eddy. Thus, the air velocity close to the surface increases with the undisturbed wind velocity, as in isothermal surfaces case.

For the air exchange velocity, however, the increase is not linear and for wall-air temperature differences above 6 K a decrease is verified from 1 to 1.5 ms^{-1}, due to the fact that, for U_0 values below a transition air velocity U_t, which is a function of wall-air temperature difference (Table 1), the turbulence term is small compared to the advective and the advective flux decreases with U_0.

To illustrate this situation Figure 4 is presented, where ΔT_w is the same (14 K) and U_0 increases, from left to right, from 1 to 1.5 ms^{-1}. For a lower U_0 (Figure 4a), the buoyancy forces are stronger than the wind induced forces, increasing the vertical mean flux comparatively to a higher U_0 (Figure 4b).

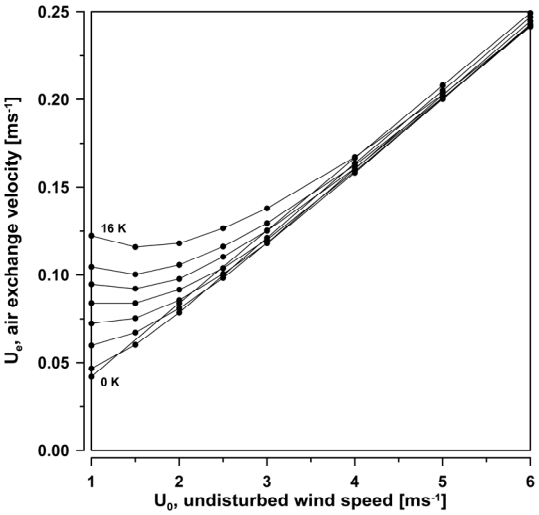

Figure 3: Air exchange velocity variation with undisturbed wind velocity for different leeward wall-air temperature difference.

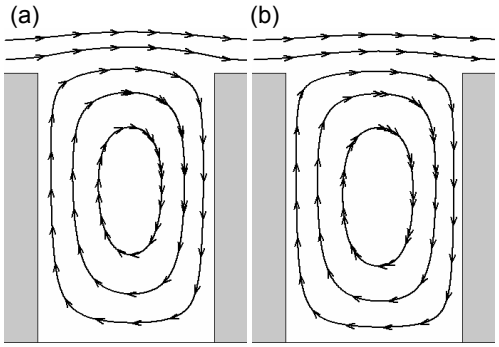

Figure 4: Air flow inside the cavity with leeward heated surface (ΔT_w=14K) and U_0: (a) 1 ms^{-1} and (b) 1.5 ms^{-1}.

5.3 Case 2: Windward heated surfaces

Windward wall heating causes the formation of a counter rotating eddy, which is annulled for U_0 above the transition air velocity. This fact explains the non linearity of the air exchange velocity as a function of U_0 shown in Figure 5, in the transition zone the air exchange velocity decreases for an increase of U_0. This is caused by an exchange of air flow regime from two counter rotating eddies (Figure 6c) to only one eddy (Figure 6d).

For an heated windward wall with an wall-air temperature difference of 14 K, when U_0 is below U_t (U_0 < 2.75 ms^{-1}), the wind induced eddy remains at the upper region and a counter rotating eddy is formed by the buoyancy forces in the center of the cavity (Figure 6a and 6b). For U_0 at the transition velocity (Figure 6c), the counter rotating eddy is restricted to the lower region and it disappears for higher U_0 (Figure 6d). This transition scheme is similar for other wall-air temperature differences, but occurs at a different U_t. The values of the transition velocity are presented in Table 1.

Table 1: Transition velocity, U_t [ms^{-1}], as a function of wall-air temperature difference for leeward and windward heated wall.

	wall-air temperature difference [K]							
	2	4	6	8	10	12	14	16
CASE1	1.5	1.5	2.0	2.0	2.0	2.0	2.0	2.0
CASE1	1.2	1.5	2.0	2.2	2.5	2.5	2.8	3.0

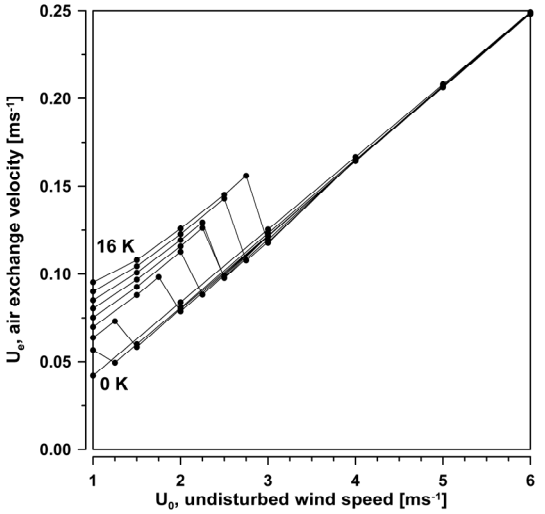

Figure 5: Air exchange velocity variation with undisturbed wind velocity for different windward wall-air temperature difference.

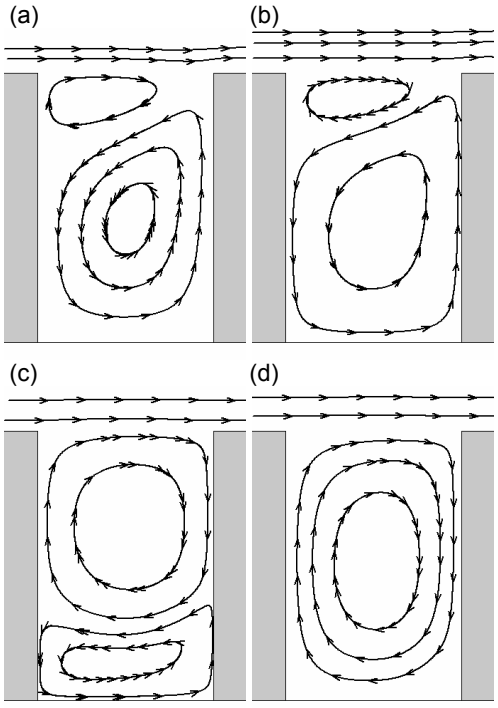

Figure 6: Air flow inside the cavity with windward heated surface (ΔT_w=14 K) and U_0: (a) 2 ms^{-1}, (b) 2.5 ms^{-1}, (c) 2.75 ms^{-1} and (d) 4 ms^{-1}.

6. AIR CAVITY MEAN TEMPERATURE

6.1 Case 1: Leeward heated surfaces

For a leeward heated wall where only the main eddy is predicted (vortex I in Figure 7a) it is expected that an increase of the eddy velocity promotes a higher heat extraction from the heated wall to the cavity air, since the heat transfer coefficient is directly proportional to air flow velocity [7]. On the other hand, an increase of air exchange velocity would increase the extraction of the heated air from the cavity to the above roof layer.

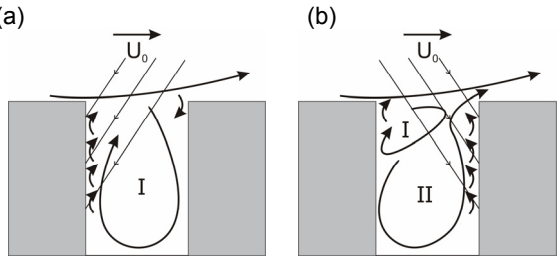

Figure 7: Air flow and heat extraction from the urban cavity with (a) leeward heated surface and (b) windward heated surface.

With this study it is verified that the air cavity mean temperature increases with the wall-air temperature difference and slightly decreases with U_0 (Figure 8). To test the variables which influence the air cavity temperature, the ratio between the air cavity mean temperature and the wall-air temperature difference ($\Delta T_c/\Delta T_w$) is plotted in Figure 9 against the ratio between air exchange velocity and the air cavity mean velocity (U_e/U_w). If a power function defined by (18) is fitted to the points above U_t of Figure 9 the following parameters are found: α = 0.008, β = -1.045 and γ = 1.014.

$$\Delta T_c = \alpha U_e^{\beta} U_w^{\gamma} \Delta T_w \quad (18)$$

Thus, it can be concluded that the mean temperature of the air cavity is correlated, for this range of U_0, with the inverse of U_e/U_w ratio, because γ is numerically close to 1 as well as the symmetric of β. Furthermore, the increase of the mean temperature of the air cavity is mainly due to:

- increase of wall temperature;
- decrease of the U_e/U_w

For U_0 below U_t, however, it is verified that the air cavity mean temperature slightly increases with U_e/U_w. For this range of U_0, the air cavity mean temperature is about 0.08 the wall-air temperature difference.

The air cavity temperature distributions, which correspond to in-cavity air flows of Figure 4, are depicted in Figure 10. When the leeward wall is heated and U_0 increased from 1 to 1.5 ms^{-1}, it is verified that the air cavity mean temperature slightly decreases (ΔT_c decreases from 1.1 K to 1.0 K).

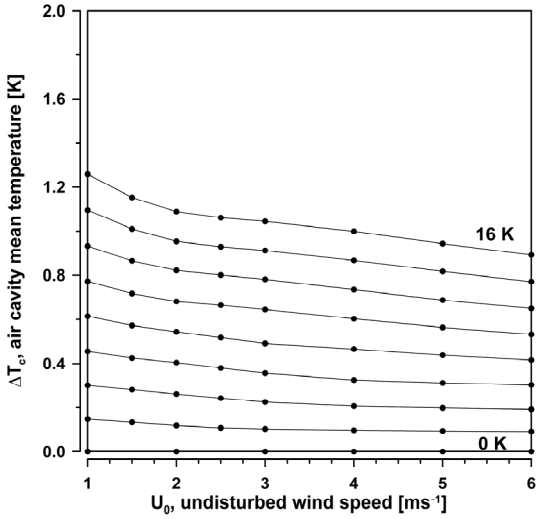

Figure 8: Air cavity mean temperature variation with undisturbed wind velocity and leeward wall-air temperature difference.

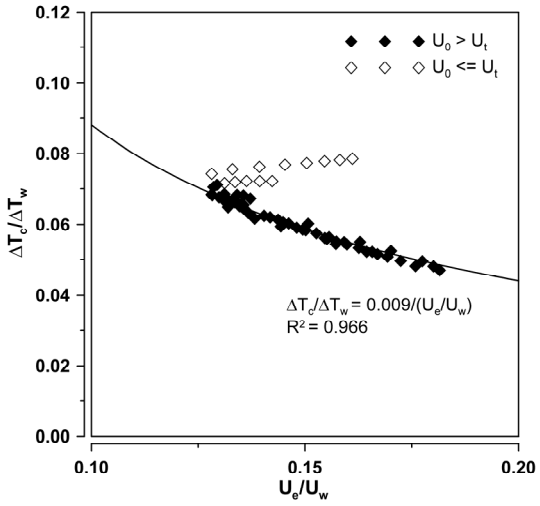

Figure 9: Ratio between the air cavity mean temperature and the wall-air temperature difference against the ratio between air exchange velocity and the cavity air velocity close to the leeward surface.

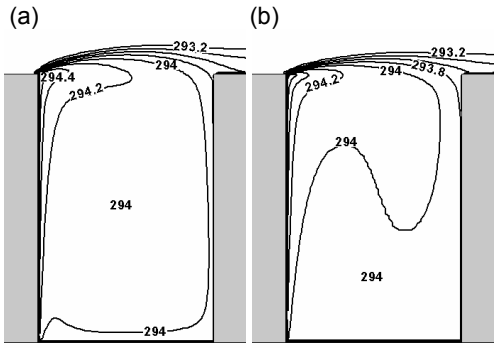

Figure 10: Temperature distribution inside the cavity with leeward heated surface (ΔT_w=14 K) and U_0: (a) 1 ms^{-1} and (b) 1.5 ms^{-1}.

6.2 Case 2: Windward heated surfaces

For a windward heated wall, one or two vortices are formed inside the cavity, depending on the undisturbed wind velocity and the wall-air temperature difference. For undisturbed wind velocity below transition velocity, the secondary counter rotating vortex (vortex II of Figure 7b) extracts heat from the wall, depending on the vortex velocity. Afterwards the heated air is removed from the right upper side of the cavity. In this case, it is difficult to predict which variables influence the heat extraction from the cavity.

For undisturbed wind velocity above the U_t value, which corresponds to the one eddy air flow regime, Figure 11 shows that the air cavity mean temperature is almost unchangeable with an increase of U_0, even if U_e increases in that region (see Figure 5). Instead, for U_0 values below U_t, it is verified that the air cavity mean temperature increases significantly with an increase of U_0. For a wall-air temperature difference of 14 K, the increase is of about 0.2 K, from 2 to 2.5 ms^{-1}, and 0.6 K from 2.5 to 2.75 ms^{-1}. The air temperature distributions for these situations are depicted in Figure 12, corresponding to the air flow regimes of Figure 6.

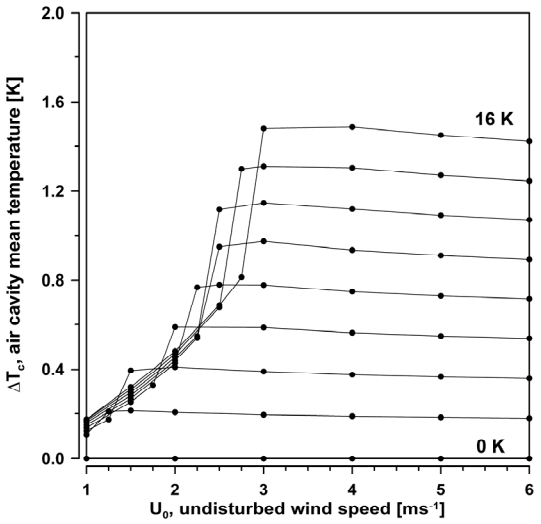

Figure 11: Air cavity mean temperature variation with undisturbed wind velocity and windward wall to air temperature difference.

The power function fitting parameters (Eq. 18) for the points where U_0 is below U_t, are α = 0.656, β = 2.122 and γ = -2.322. So, it is concluded that, for this range of U_0 values, the air cavity mean temperature increases with the quadratic function of U_e/U_w as Figure 13 shows. When U_0 is above U_t, $\Delta T_c/\Delta T_w$ varies between 0.09 and 0.11 K, which means that for a 10K increase on the wall temperature it is predicted that the temperature inside the cavity increases about 1 K.

From Figures 9 and 13, it can be concluded that the highest heat accumulation is verified when windward wall is heated and U_0 is above the transition velocity, U_t. In fact, for an air flow regime where the advective vortex is dominant, the in-cavity air is like 'isolated' from the above roof level and the downward air is heated when it contacts with the windward

surface. The heated air is then transported inside the cavity by the main air flow vortex (Figure 12c and 12d). On the other hand, the air flow regime where the main vortex is caused by buoyancy, which occurs when windward wall is heated and U_0 is below U_t, is the most favorable case to the heat extraction from the cavity (Figure 12a and 12b). The upward air movement extracts the heated air close to the surface, with little influence on the air cavity temperature.

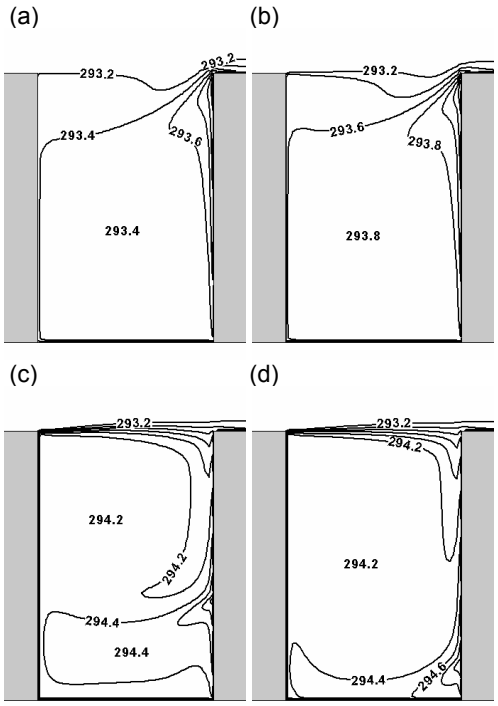

Figure 12: Temperature distribution inside the cavity with windward heated surface (ΔT_w=14 K) and U_0: (a) 2 ms^{-1}, (b) 2.5 ms^{-1}, (c) 2.75 ms^{-1} and (d) 4 ms^{-1}.

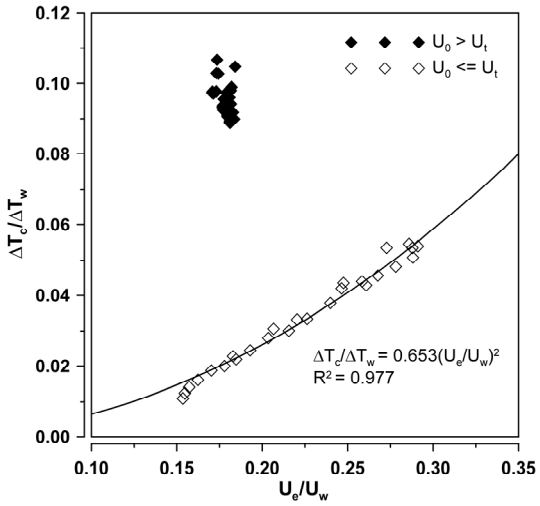

Figure 13: Ratio between the air cavity mean temperature and the wall-air temperature difference against the ratio between air exchange velocity and the cavity air velocity close to the windward surface.

7. CONCLUSIONS

This study evidences that thermal spatial differences among surfaces can be determinant for the air flow regime inside the urban cavity, caused by the balance between buoyancy and advective forces, which depends on the undisturbed wind velocity and the position of the heated wall.

When the heated wall is facing the wind direction (windward heated wall), two different air flow regimes are predicted by the model. Below the transition velocity, which is a function of wall-air temperature difference, two eddies are formed. This case is favorable to extract heat from the cavity and the air cavity mean temperature increases with an increase of the ratio between the air exchange velocity and the air velocity close to the heated surface. Above the transition velocity, only the wind induced eddy is predicted and the heated air is hardly extracted from the cavity. For each 10 K increase of the wall temperature, an increase of 1 K is verified in the in-cavity air. On the other hand, when the heated wall is facing the opposite direction to the wind (leeward heated wall), independently of the undisturbed wind velocity value, only the wind induced eddy is formed, induced by the upward heated air. In terms of air cavity mean temperature, this case is intermediate relatively to the other two. An increase of 10 K in the wall temperature results in an increase from 0.5 K to 0.8 K in the in-cavity air.

ACKNOWLEDGEMENT

The authors acknowledge the contribution of the Portuguese National Foundation of Science and Technology of the Ministry for Science and Technology by supporting Marta J. N. Oliveira Panão with a PhD Grant (SFRH/BD/12256/2003).

REFERENCES

[1] J.F. Sini, S. Anquetini, P. Mestayer, Pollutant Dispersion and Thermal Effects in Urban Street Canyons, Atmos. Environ., 30 (15) (1996), 2659.

[2] J.J. Kim, J.J. Baik, A Numerical Study of Thermal Effects on Flow and Pollutant Dispersion in Urban Street Canyons, J.Appl. Meteorol., 38 (1999), 1249.

[3] T.R. Oke, Street Design and Urban Canopy Layer Climate, Energy and Buildings, 11 (1988), 103.

[4] C.-H. Liu, D. Leung, M.C. Barth, On the Prediction of air and Pollutant Exchange Rates in Street Canyons of Different Aspect Ratios Using Large-Eddy Simulation, Atmos. Environ., 39 (2005), 1567.

[5] A.D. Gosman and F.J.K Ideriah, F.J.K., TEACH-T: A General Computer Program for Two-dimensional, Turbulent, Recirculating Flows. Dept. of Mechanical Engineering, Imperial College, London, 1976.

[7] H. Versteeg and W. Malalasekera, An Introduction to Computational Fluid Dynamics, Ed. Longman Scientific and Technical, Essex, Uk, 1995.

[8] G. Mills, Simulation of the Energy Budget of an Urban Canyon – I. Model Structure and Sensivity Test, Atmospheric Environment, 27B (1993), 157.